Journal of Biomedical Optics

SPIEDigitalLibrary.org/jbo

Near-infrared-excited confocal Raman spectroscopy advances *in vivo* diagnosis of cervical precancer

Shiyamala Duraipandian
Wei Zheng
Joseph Ng
Jeffrey J. H. Low
Arunachalam Ilancheran
Zhiwei Huang

SPIE

Near-infrared-excited confocal Raman spectroscopy advances *in vivo* diagnosis of cervical precancer

Shiyamala Duraipandian,[a] Wei Zheng,[a] Joseph Ng,[b] Jeffrey J. H. Low,[b] Arunachalam Ilancheran,[b] and Zhiwei Huang[a]
[a]National University of Singapore, Department of Bioengineering, Faculty of Engineering, Optical Bioimaging Laboratory, 117576, Singapore
[b]National University Hospital and National University of Singapore, Department of Obstetrics and Gynecology, Division of Gynecologic Oncology, 119074, Singapore

Abstract. Raman spectroscopy is a unique optical technique that can probe the changes of vibrational modes of biomolecules associated with tissue premalignant transformation. This study evaluates the clinical utility of confocal Raman spectroscopy over near-infrared (NIR) autofluorescence (AF) spectroscopy and composite NIR AF/Raman spectroscopy for improving early diagnosis of cervical precancer *in vivo* at colposcopy. A rapid NIR Raman system coupled with a ball-lens fiber-optic confocal Raman probe was utilized for *in vivo* NIR AF/Raman spectral measurements of the cervix. A total of 1240 *in vivo* Raman spectra [normal ($n = 993$), dysplasia ($n = 247$)] were acquired from 84 cervical patients. Principal components analysis (PCA) and linear discriminant analysis (LDA) together with a leave-one-patient-out, cross-validation method were used to extract the diagnostic information associated with distinctive spectroscopic modalities. The diagnostic ability of confocal Raman spectroscopy was evaluated using the PCA-LDA model developed from the significant principal components (PCs) [i.e., PC4, 0.0023%; PC5, 0.00095%; PC8, 0.00022%, ($p < 0.05$)], representing the primary tissue Raman features (e.g., 854, 937, 1095, 1253, 1311, 1445, and 1654 cm^{-1}). Confocal Raman spectroscopy coupled with PCA-LDA modeling yielded the diagnostic accuracy of 84.1% (a sensitivity of 81.0% and a specificity of 87.1%) for *in vivo* discrimination of dysplastic cervix. The receiver operating characteristic curves further confirmed that the best classification was achieved using confocal Raman spectroscopy compared to the composite NIR AF/Raman spectroscopy or NIR AF spectroscopy alone. This study illustrates that confocal Raman spectroscopy has great potential to improve early diagnosis of cervical precancer *in vivo* during clinical colposcopy. [DOI: 10.1117/1.JBO.18.6.067007]

Keywords: cervical dysplasia; near-infrared; autofluorescence; confocal Raman spectroscopy; *in vivo* diagnosis.

Paper 130086R received Feb. 14, 2013; revised manuscript received May 18, 2013; accepted for publication May 21, 2013; published online Jun. 24, 2013.

1 Introduction

Cervical cancer is the second most common malignancy in women worldwide.[1] Early detection and localization of precancer in the cervix with effective treatment is crucial to improving the survival rates of the patients at high risk. The conventional exfoliative cervicovaginal cytology [i.e., Papanicolaou (Pap) smear] tests have high diagnostic specificity of 93% [95% confidence interval (CI): 89 to 97%], but with a relatively low sensitivity of 57% (95% CI: 38 to 76%) for the diagnosis of precancerous lesions in the cervix.[2] The white-light colposcopy, the common gynecology follow-up for abnormal Pap smears, has a good sensitivity of ~96%, but this is tempered by a mediocre detection specificity of ~48% for identifying preneoplastic changes in the cervix.[2,3] While histological identification of cervical precancer and cancer remains the gold standard diagnostic approach, it is impractical as a routine screening tool for high-risk patients who may have multiple suspicious lesions. Therefore, the development of advanced optical diagnostic techniques for improving both the diagnostic sensitivity and specificity is clinically imperative for real-time, accurate diagnosis of cervical precancer *in vivo*.

Address all correspondence to: Zhiwei Huang, National University of Singapore, Department of Bioengineering, Faculty of Engineering, Optical Bioimaging Laboratory, 9 Engineering Drive 1, 117576, Singapore. Tel: +65 6516 8856; Fax: +65 6872 3069; E-mail: biehzw@nus.edu.sg

Among different optical spectroscopic techniques, near-infrared (NIR) Raman spectroscopy has been recognized as an excellent technique with high biomolecular specificity for *in vitro* and *in vivo* diagnosis of malignancies in various organs including in the cervix.[4–11] NIR Raman spectroscopy is a molecule-specific technique for optically probing the vibrations of biomolecules, revealing the highly specific biochemical structures and conformations of tissue and cells. However, Raman signal emanating from tissue is inherently very weak and occurs concurrently with the intense tissue autofluorescence (AF) background. The tissue NIR AF background typically represents the light re-emission from the excited endogenous fluorophores. NIR AF has shown promise in differentiating cancer from normal tissues, probably due to the neoplasia-associated changes in tissue absorption, scattering, or endogenous fluorophore content and distribution in tissue.[4,12] NIR-excited spectroscopy holds potential benefits for safe tissue diagnosis, such as noncarcinogenic and relatively insensitive to tissue water content, compared to the ultraviolet-visible-excited spectroscopy. For instance, the diagnostic capability of the composite NIR AF/Raman spectroscopy together with principal components analysis (PCA) and linear discriminant analysis (LDA) for enhancing the assessment of *in vivo* skin tumors was demonstrated using mice tumor models.[12] We have also documented the complementary nature of NIR AF and Raman spectroscopy techniques using a volume-type Raman endoscopic probe[13] and found that

combining NIR AF and Raman modalities improved the gastric cancer diagnosis *in vivo* during gastroscopic inspections.[4] The diagnostic potential of *in vitro* NIR AF imaging, as well as *in vivo* NIR AF spectroscopy, for colonic cancer and precancer detection have also been reported very recently.[8,14,15] However, to date, no systematic studies have been conducted to investigate the diagnostic utility of confocal Raman, NIR AF and the composite NIR AF/Raman spectroscopy for cervical precancer detection. In this work, we use a ball-lens confocal Raman probe, which was developed to acquire spectroscopic information about cervical tissue *in vivo*. We compare the diagnostic performance of the three spectroscopic modalities (i.e., confocal Raman, NIR AF, and the composite NIR AF/Raman spectroscopy) using PCA-LDA-based diagnostic algorithms and confirm that confocal Raman spectroscopy is the most robust means for improving *in vivo* diagnosis of cervical precancer at colposcopy.

2 Materials and Methods

2.1 *Raman Instrumentation*

The confocal Raman spectroscopy system used for *in vivo* tissue NIR AF and Raman measurements has been reported in detail elsewhere.[9] Briefly, the system consists of an external cavity-stabilized 785-nm diode laser (maximum output: 300 mW, B&W TEK Inc., Newark, DE), a high-throughput spectrometer (QE65000, Ocean Optics Inc., Dunedin, FL) equipped with an NIR-enhanced, back-thinned charge-coupled device (CCD) detector (S7031-1006, 1024×58 with pixel sizes of 24.6 μm, QE>90%, Hamamatsu, Shizuoka, Japan), and a specially designed hand-held fiber-optic confocal Raman probe coupled with a ball-lens (5 mm in diameter, refractive index $n = 1.77$, NA = 1.5) at the tip.[9,16] The 785-nm laser light with a power of ~10 mW on the probe tip and a beam size of ~0.2 mm was focused onto the tissue surface during the clinical spectral measurements. The optical configuration of the depth-selective Raman probe has been described in detail in Ref. 9. The probe consists of an illumination and collection arm integrated with two stages of optical filtering. The filtering modules are incorporated at the proximal and distal ends of the probe to remove fiber fluorescence, silica Raman signals, and Rayleigh scattered light, while allowing only the frequency-shifted tissue Raman signal to pass. The coupling of an NIR-coated sapphire ball-lens with the bifurcated fiber-optic Raman probe offers a high degree of confocality for depth-selective tissue excitation as well as back-scattered tissue Raman photons collection. Monte Carlo simulations showed that the confocal Raman probe developed can selectively maximize the collection of epithelial tissue Raman photons (~160 μm),[9,16] while reducing the detection of emitted photons from deeper tissue layers (i.e., strong stromal AF), as compared to the volume fiber-optic Raman probe.[13] All the optics of the Raman probe are sealed into the stainless steel sleeve (outer diameter of 8 mm) with a polytetrafluoroethylene gasket. The system acquires the composite NIR AF/Raman spectra in the fingerprint region (800 to 1800 cm^{-1}) from *in vivo* cervical tissue and each spectrum is acquired within 1 s with a spectral resolution of ~8 cm^{-1}. The atomic emission lines of mercury-argon spectral calibration lamps (HG-1 and AR-1, Ocean Optics Inc., Dunedin, FL) are used for wavelength calibration. All the wavelength-calibrated composite NIR AF/Raman spectra are also corrected for the wavelength-dependence of the system using a tungsten-halogen calibration lamp (RS-10, EG&G Gamma Scientific, San Diego, CA).

2.2 *Patients*

A total of 84 nonpregnant female patients (between 18 and 70 years of age) who underwent colposcopic examination due to abnormal Pap smears were enrolled in colposcopy clinic at the National University Hospital (NUH), Singapore. All patients preoperatively signed an informed consent, permitting the investigative collection of *in vivo* spectroscopic measurements on the cervix. This study was approved by the Ethics Committee of the National Healthcare Group of Singapore. Prior to spectroscopic measurements, a complete routine colposcopic examination was performed on the patients by experienced colposcopists. A 5% acetic acid is applied to the cervix to create a distinct demarcation between normal and abnormal epithelium by inducing the transient whitening changes in the cervical epithelium.[17,18] The fiber-optic confocal Raman probe was eventually advanced through the speculum and placed in gentle contact with the cervix. The *in vivo* composite NIR AF/Raman spectra were subsequently measured from both abnormal (i.e., acetowhite epithelium) and the surrounding normal ectocervical squamous epithelial sites identified by the experienced colposcopists (i.e., the normal tissue does not exhibit color patterned changes that only accompany dysplastic epithelium).[6] Hereafter, the colposcopically normal-looking tissue sites were referred to as normal and no biopsies were taken from these cervical tissue sites. Multiple Raman spectral measurements (~7 to 9) were taken on each site of the cervical tissue (~2 to 3 sites per patient) for evaluation of inter- and/or intratissue variability of the subjects. As a result, a total of 1240 *in vivo* composite NIR AF/Raman spectra were measured from the cervixes of the 84 patients recruited, in which 993 spectra were acquired from 115 normal sites, whereas 247 spectra were from 25 high-grade precancerous lesions. After the spectral acquisition, colposcopy-guided punch biopsies were taken from the abnormal tissue sites measured and sent for histopathology confirmation. The histopathology results served as the gold standard for evaluating the performance of spectroscopic techniques for *in vivo* cervical precancer diagnosis. Note that among different cervical tissue pathologies, high-grade dysplastic lesions have extremely important clinical implications as these clinically silent precancerous lesions are at high risk of progressing into cancer in the absence of treatment. Hence, molecular-level detection of these high-grade lesions is of paramount importance to reduce their prevalence.

2.3 *Data Preprocessing*

The *in vivo* composite NIR AF/Raman spectra acquired from the cervix in the 800 to 1800 cm^{-1} range represented a combination of prominent tissue AF background, weak tissue Raman scattered signals, and noise. Subsequent spectral preprocessing such as CCD dark-noise subtraction, system spectral response calibration, tissue AF background subtraction (fifth-order polynomial fit), and laser power normalization were performed on the measured spectra. The spectral preprocessing and diagnostic algorithms were completed on-line and displayed in a real-time interactive graphical user interface together with the diagnostic outcomes.[19]

2.4 *Multivariate Statistical Analysis*

Direct implementation of statistical analysis (e.g., LDA, etc.) on the high-dimensional composite NIR AF/Raman spectral dataset may lead to inefficient disease classification.[4] Hence, PCA is initially employed to reduce the spectral space through the identification of a reduced number of orthogonal principal components (PCs), and then the PCs are arranged in descending order of variance as explained. The PCs preserve most of the total variance in the spectral datasets for effective tissue classification, while eliminating the redundant information. In this study, the diagnostic information contained in the PCs can be perceived in the context of identifying the discriminating features in the underlying spectroscopic data associated with distinct spectroscopic modalities.[4] The identified significant PCs ($p < 0.05$) were then fed to the LDA classifiers for effective disease identification. LDA determines the discriminant function that maximizes the variance between the groups, while minimizing the variance within a group. The performance of the diagnostic algorithms rendered by the PCA-LDA models for predicting different tissue pathologies (e.g., normal, precancer) was validated in an unbiased manner using leave-one-patient-out, cross-validation method. The receiver operating characteristic (ROC) curves were further generated to determine the robustness of PCA-LDA models for correct and incorrect tissue classifications. The spectral analysis was performed using in-house written Matlab scripts (Mathworks Inc., Natick, MA).

3 Results

Figure 1 shows the mean *in vivo* composite NIR AF/Raman, NIR AF, and NIR Raman spectra [Fig. 1(a), 1(c), and 1(e)] together with the corresponding difference spectra [Fig. 1(b), 1(d), and 1(f)], collected from normal ($n = 993$) and precancerous ($n = 247$) cervical tissues of 84 patients recruited under the guidance of white-light colposcopy. The composite NIR AF/Raman spectra [Fig. 1(a)] exhibit intense, broad but overall decreasing AF intensity curves [fifth-order polynomial fit, Fig. 1(c)] with the superimposed prominent tissue Raman bands [Fig. 1(e)]. The major Raman peaks observed in both normal and precancer cervical tissues are at the following positions with tentative biochemical assignments: 854 cm^{-1} {glycogen [(CCH) deformation-aromatic] and (C-C) stretching of

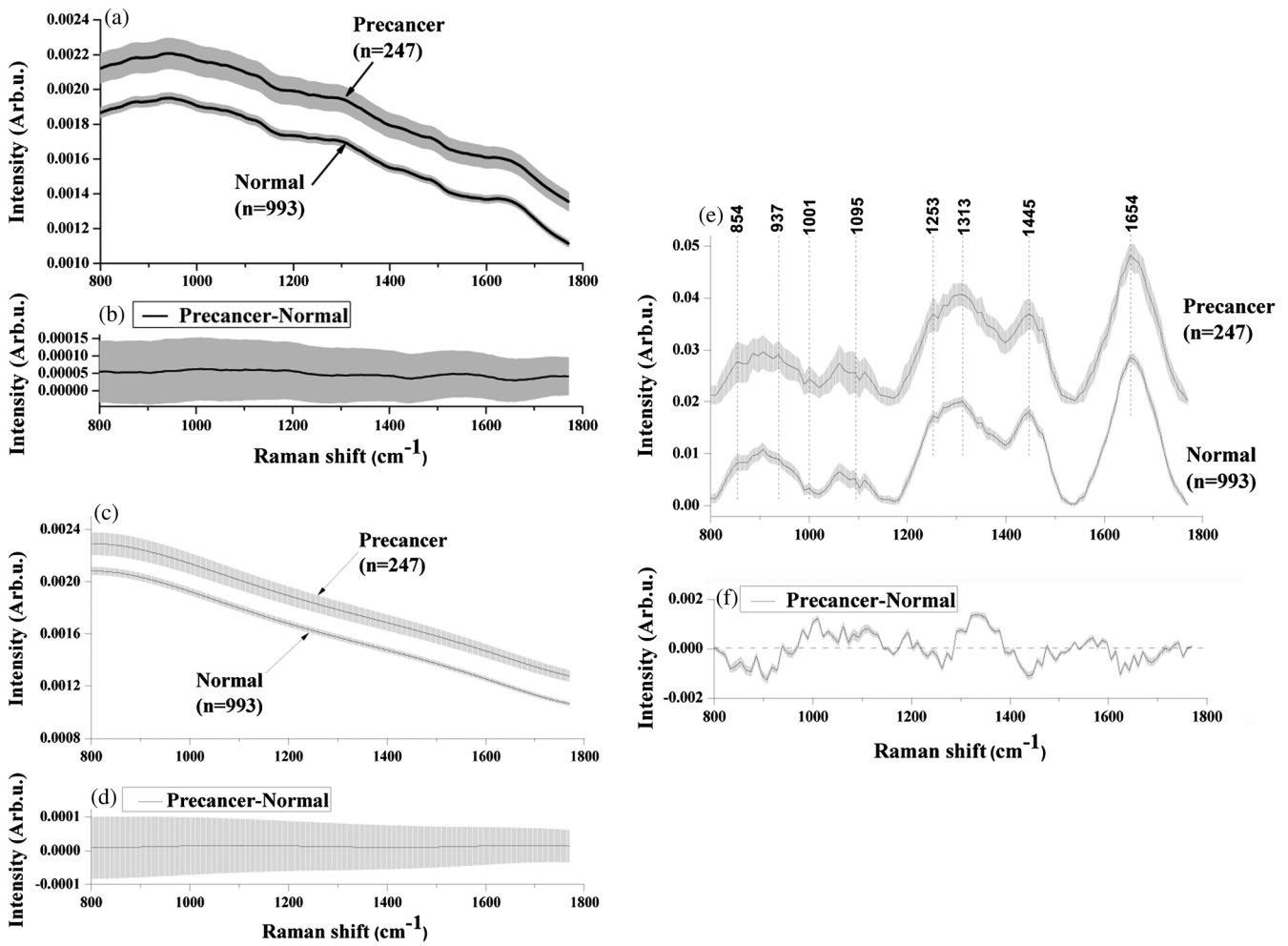

Fig. 1 (a) The mean *in vivo* composite NIR AF and Raman spectra ±1 standard errors (SE) and (b) the corresponding mean difference spectrum ±1 SE from normal ($n = 993$) and precancer ($n = 247$) cervical tissue, (c) the mean *in vivo* NIR AF spectra ±1 SE and (d) the mean difference spectrum ±1 SE from normal ($n = 993$) and precancer ($n = 247$) cervical tissue, (e) the mean *in vivo* NIR Raman spectra ±1 SE and (f) the mean difference spectrum ±1 SE from normal ($n = 993$) and precancer ($n = 247$) cervical tissue. The mean *in vivo* spectra of precancer cervical tissue were shifted vertically for better visualization. The shaded area represents the respective SE. Note that the SE of precancer and normal Raman signals in Fig. 1(e) have been magnified by 20-fold for better visualization.

structural proteins and collagen}, 937 cm^{-1} (stretching of proline, valine, and glycogen), 1001 cm^{-1} [(C—C) ring breathing of phenylalanine], 1095 cm^{-1} (DNA phospholipids backbone), 1253 cm^{-1} (amide III), 1313 cm^{-1} (CH_3CH_2 twisting mode of lipids/proteins), 1445 cm^{-1} (CH_2 bending mode of proteins and lipids), and 1654 cm^{-1} [amide I band, (C=O) stretching mode of proteins].[7,10,20–22] The comprehensive biomolecular basis of Raman spectroscopic diagnosis of cervical dysplasia has been described in detail elsewhere.[7,9,22] The AF spectra show higher intensity for dysplasia; however, the change in AF intensity associated with dysplastic progression was not significant ($p = 0.924$), indicating that the confocal-based NIR AF spectroscopy is inefficient for precancer identification. Conversely, the intensity of Raman-active tissue biochemical constituents changed significantly ($p < 0.05$) with precancer transformation. For instance, the dysplastic tissue showed increased Raman signals at 1001, 1095, and 1313 cm^{-1}, but exhibited much lower signals at 854, 937, 1253, 1445, and 1654 cm^{-1} as compared to the normal tissue.[6,7,20–23] These striking differences in the Raman-active components between different tissue pathologies indicate the diagnostic potential of confocal Raman spectroscopy for rapid *in vivo* diagnosis of precancer and early cancer in the cervix.

PCA-LDA-based multivariate diagnostic algorithms were subsequently rendered on the composite NIR AF/Raman spectra measured to extract the diagnostic information associated with underlying spectroscopy modalities (i.e., confocal Raman, NIR AF, and the composite NIR AF/Raman) for discrimination between dysplasia and normal cervical tissues. The composite NIR AF/Raman spectra were mean centered to eliminate the common variance. Hotelling T^2 and Q-residuals were employed to remove the spectra with unusual line shape variations due to noncontact measurements and probe handling variations.[19] Figure 2 shows the diagnostically significant PC loadings [PC4, 0.0023%; PC5, 0.00095%; PC8, 0.00022%, ($p < 0.05$)], representing the variations in the major tissue Raman peaks (e.g., 854, 937, 1095, 1253, 1311, 1445, and 1654 cm^{-1}) together with PC1 (99.93%, $p = 0.924$), typically exhibiting

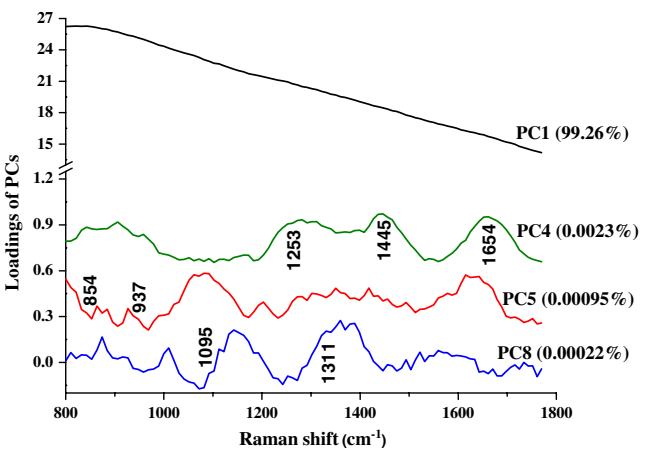

Fig. 2 Principal components (PCs) loadings calculated from the *in vivo* composite NIR AF/Raman spectra of cervical tissue, revealing the diagnostically significant spectral features for tissue classification. The three diagnostically significant PCs (PC4, 0.0023%; PC5, 0.00095%; PC8, 0.00022%) accounting for about 0.00347% of total variance represented the major tissue Raman peaks. PC1 (99.93%) showed the tissue AF features. The loading on PC1 has been magnified by 200-fold for better visualization.

the broad tissue NIR AF features. LDA classifier was further employed on the diagnostically significant PCs, and the cross-validated classification results for each spectrum belonging to normal and precancer tissue categories were obtained (Fig. 3). The PC1 constituting the tissue AF features rendered a diagnostic accuracy of 59.6% [sensitivity of 49.8% (123/247) and specificity of 69.4% (689/993)]. A diagnostic accuracy of 84.1% [sensitivity of 81.0% (200/247) and specificity of 87.1% (865/993)] could be achieved using PC4, PC5, and PC8, primarily describing the significant tissue Raman spectral features (e.g., 854, 937, 1095, 1253, 1311, 1445, and 1654 cm^{-1}). The PCs representing tissue AF (PC1) as well as Raman features (PC4, PC5, and PC8) were combined together to assess the diagnostic ability of the composite NIR AF/Raman spectroscopy modality, achieving a diagnostic accuracy of 82.3% [sensitivity of 76.9% (190/247) and specificity of 87.7% (871/993)]. In addition, the diagnostic performance of the three spectroscopic modalities was further evaluated by splitting the total dataset into a training set (70% of the total dataset) and a testing set (30% of the total dataset). The redeveloped PCA-LDA models using the PCs representing tissue Raman, the composite NIR AF/Raman, and NIR AF features provided predictive accuracies of 86.1% (95% CI: 83.6 to 88.7%), 85.7% (95% CI: 80.5 to 90.8%), and 59.8% (95% CI: 52.6 to 66.9%) for cervical precancer classification, respectively.

ROC curves were also generated (Fig. 4) to further compare the performance of the PCA-LDA-based diagnostic algorithms developed from the three spectroscopic modalities (confocal Raman, the composite NIR AF/Raman, and NIR AF) for *in vivo* tissue classification. The areas under the ROC curves (AUC) were 0.88, 0.86, and 0.56 for the PCA-LDA models developed from the confocal Raman, the composite NIR AF/Raman, and NIR AF models, respectively, indicating that the diagnosis achieved using the confocal Raman diagnostic modality was superior to NIR AF spectroscopy, but marginally higher than the composite NIR AF/Raman spectroscopy.

4 Discussion

In the past decade, substantial research efforts have been made to develop advanced optical spectroscopy modalities for noninvasive *in vivo* detection of cervical precancer and cancer. In particular, Raman spectroscopy is a unique molecular vibrational technique that has found its remarkable way into routine clinical oncology applications because of its excellent capability of nondestructively probing the changes of biochemical vibrational markers associated with dysplastic transformation. The dysplastic cells initially develop in the epithelium, such that the targeted confocal illumination and collection of signals originating from the epithelial layer in the cervix is essential to improving Raman spectroscopic diagnosis of precancer. Hence, in this study, we utilize a ball-lens confocal Raman probe to selectively measure the *in vivo* composite NIR AF/Raman spectra, which exhibit the spectral contributions primarily from the epithelial layer of the cervix. Consequently, it can reveal the alterations in the Raman-active molecules related to metabolic changes in the cervical epithelium, while minimizing AF contributions from deeper stromal tissue layer.[9,16,24]

The PCA-LDA modeling was performed on the composite NIR AF/Raman spectra measured to extract the PC loadings related to tissue NIR AF (an intense decreasing broad band curve) and Raman features (highly specific tissue biochemical

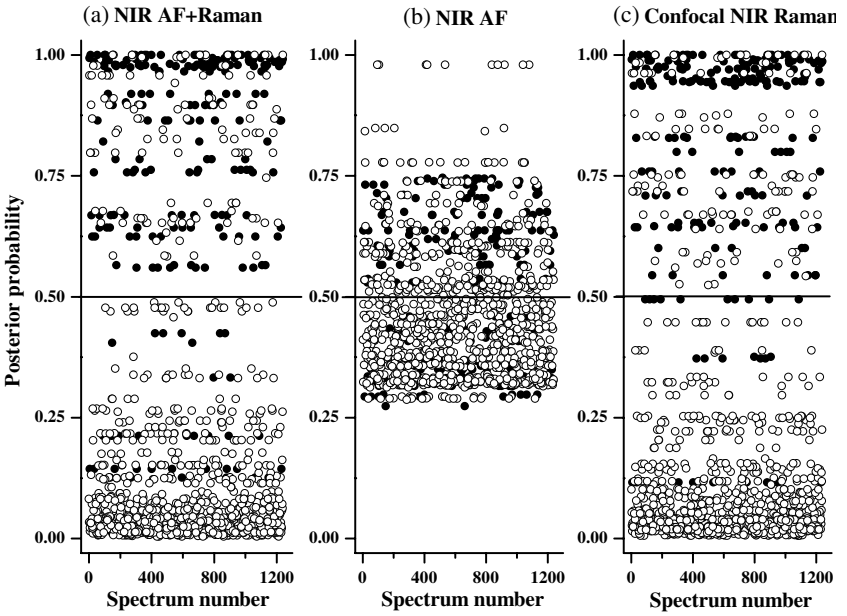

Fig. 3 Scatter plots of the posterior probability of belonging to normal and precancer categories calculated from the three spectroscopic modalities: (a) composite NIR AF/Raman (PC1, PC4, PC5, PC8); (b) NIR AF (PC1); (c) confocal Raman spectra (PC4, PC5, PC8); (•) Precancer ($n = 247$), (○) Normal ($n = 993$).

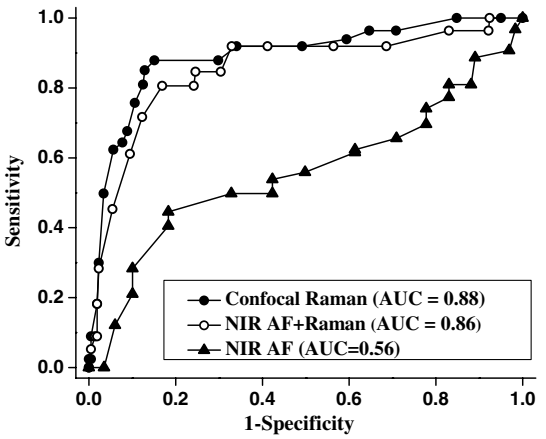

Fig. 4 Receiver operating characteristic (ROC) curves of discrimination results for cervical precancer classification using *in vivo* confocal Raman, the composite NIR AF/Raman, and NIR AF spectroscopy, respectively, together with PCA-LDA and leave-one patient-out, cross-validation methods. The areas under the ROC curves are 0.88, 0.86, and 0.56 for the confocal Raman, composite NIR AF/Raman, and NIR AF spectroscopy modalities, respectively.

fingerprints), resolving the diagnostic features associated with distinctive spectroscopy modalities. The NIR AF spectra of dysplasia tissue exhibited higher intensity than normal cervical tissue, which was in agreement with the literature.[12,25] However, the origin of NIR AF is not yet well documented. Porphyrin is assumed to be one of the major fluorophores in the NIR region[25]. The increase of tissue NIR AF with precancer progression could be correlated to the elevated level of porphyrins in cancer or precancer tissue, which has been observed in human breast and bladder tissue,[25,26] as well as animal tumor models.[12,27] The increase of porphyrins in the tumor tissue is probably due to necrosis, microbial contamination of tumor tissue, or the ability to concentrate porphyrins by some types of cells of epithelial origin.[26,28] The hypervascularization in the precancer tissue could also contribute to the increased level of porphyrins.[12] The increase of epithelial fluorescence in dysplasia tissue could also be related to changes of other endogenous fluorophores (e.g., reduced nicotinamide adenine dinucleotide and flavin adenine dinucleotide) with the development of dysplasia in cervical tissue.[29–31] The change in NIR AF spectral line shape was captured by PC1, accounting for the largest percentage of total variance (99.93%). PC1 suggested that the increased NIR AF emission associated with precancer progression was insignificant ($p = 0.924$), indicating that the change in the concentration of NIR endogenous fluorophores probed from the epithelial tissue using the confocal Raman probe was inefficient for discriminating the dysplastic lesions from the normal cervical tissue. This resulted in the very poor diagnostic accuracy of 59.6% [sensitivity of 49.8% (123/247) and specificity of 69.4% (689/993)] using the confocal NIR AF spectroscopy (PC1 associated with tissue AF changes) (Fig. 3). The PCA-LDA model developed using the PCs [PC4, 0.0023%; PC5, 0.00095%; PC8, 0.00022% ($p < 0.05$)] representing the highly specific tissue Raman signatures was able to extract the diagnostic information related to the molecular changes in dysplastic cervix. These distinctive and significant variations ($p < 0.05$) in the relative intensities of Raman bands accompanying dysplastic transformation can be instantly correlated to the changes of tissue biochemical compositions. For instance, the spectra showed decreased glycogen and structural proteins (854 cm^{-1}), primarily representing the loss of epithelial cell differentiation during neoplastic progression.[22,32] The increased nuclear content (1095 cm^{-1}) indicated the elevated number of epithelial cells in the dysplastic cervix.[22,32,33] The amide I (1654 cm^{-1}) and amide III (1253 cm^{-1}) bands were also noticeably decreased with dysplastic transformation.[33] Hence, the diagnostic model developed using these changes in the concentration of Raman-active biomolecules associated with dysplastic progression yielded the diagnostic accuracy of 84.1% [a sensitivity of 81.0%

(200/247) and a specificity of 87.1% (865/993)] (Fig. 3), illustrating the diagnostic utility of confocal Raman spectroscopy for *in vivo* cervical precancer diagnosis at the molecular level.

We also examined if the cocontributions of the composite NIR AF and confocal Raman spectroscopy could improve the precancer detection compared to confocal Raman spectroscopy alone. The PCA-LDA model was redeveloped by combining the PCs constituting the features of both NIR AF and Raman spectroscopy modalities (PC1, PC4, PC5, and PC8). The combined NIR AF/Raman diagnostic model achieved the accuracy of 82.3% with a sensitivity of 76.9% (190/247) and a specificity of 87.7% (871/993) (Fig. 3), which was marginally reduced compared to the diagnostic ability of confocal Raman spectroscopy. This indicates that confocal Raman spectroscopy can be used as a standalone diagnostic modality for identifying the dysplastic cervix in clinical colposcopy. On the other hand, to better understand the ability of confocal Raman spectroscopy for improving cervical precancer diagnosis, we have compared the tissue NIR AF/Raman spectra acquired from a two-layer tissue model[24] using both the ball-lens confocal Raman probe and a volume Raman probe under the 785-nm excitation light. The result[24] shows that the volume Raman probe measures ~74% NIR AF/Raman signals emanating from deeper tissue layer. In contrast, the ball-lens confocal Raman probe detects ~80% of NIR AF/Raman signals originating from the superficial layer of the two-layer tissue model, confirming that confocal Raman spectroscopy technique is highly favorable for early detection of epithelial precancer *in vivo*. Unlike our previous gastric Raman study that used a volume Raman probe for improving gastric cancer diagnosis,[4] the combined NIR AF and Raman spectroscopy using confocal probe in this study does not much improve the *in vivo* diagnosis of cervical precancer (Figs. 3 and 4). The diagnostic differences could be due to the following reasons: (1) in gastric Raman study,[4] we applied a volume Raman probe to investigate gastric cancer tissue whereby the proliferating cancer cells invaded the underlying basement membrane and stromal layer. The reduction in stromal collagen and AF reabsorption due to excessive angiogenesis in cancer tissue can result in a decrease of NIR AF associated with gastric cancer. Thus the volume Raman probe, particularly in favor of probing the deeper tissue changes, can be used to improve the detection of AF changes of deeper layer tissue (e.g., collagen in stromal tissue, vascular information) associated with gastric cancer. (2) In the current study, we targeted at detecting cervical dysplasia which were largely confined to the epithelium (i.e., within the basement membrane) in the cervix. A confocal Raman probe is specially designed in favor of probing the biochemical changes of superficial epithelial layer (rather than the deeper tissue layer). However, the change of AF spectra of dysplastic tissue is mostly occurring in the deeper connective tissue adjacent to epithelium,[29,34] which results in an inefficiency when using confocal Raman probe for probing the AF changes of deeper cervical tissue associated with precancer transformation. One notes that the balanced accuracy $[(\text{sensitivity} + \text{specificity})/2]$ is computed in this study due to the unbalanced dataset (a large number of true negatives).[35] The ROC curves further confirm the best diagnostic performance of confocal Raman spectroscopy (AUC, 0.88) (Fig. 4) compared to NIR AF (AUC, 0.56) or composite NIR AF/Raman spectroscopy (AUC, 0.86) for cervical precancer identification. Overall, the results show that confocal Raman spectroscopy in conjunction with PCA-LDA modeling holds a great promise as a diagnostic tool for improving the detection of subtle biomolecular changes in dysplastic lesions leading to early cervical cancer. Currently, further clinical trials on a larger number of cervical patients with different pathological groups (e.g., low-grade/high-grade dysplasia, squamous metaplasia) are in progress at NUH for evaluating the true clinical merits of confocal Raman technique for improving the early diagnosis of cervical precancer and cancer in obstetrics and gynecology clinic.

In summary, this study demonstrates that NIR-excited confocal Raman spectroscopy can be used for improving precancer diagnosis by selectively probing dysplasia-associated molecular changes primarily from epithelial tissue. Hence, confocal Raman spectroscopy technique has the potential to become a powerful diagnostic tool in adjunct to colposcopy for cervical precancer and early cancer detection *in vivo* during clinical colposcopic examination.

Acknowledgments

This research was supported by the National Medical Research Council and the Biomedical Research Council, Singapore.

References

1. D. M. Parkin et al., "Estimating the world cancer burden: Globocan 2000," *Int. J. Cancer* **94**(2), 153–156 (2001).
2. M. Arbyn et al., "Pooled analysis of the accuracy of five cervical cancer screening tests assessed in eleven studies in Africa and India," *Int. J. Cancer* **123**(1), 153–160 (2008).
3. M. F. Mitchell et al., "Colposcopy for the diagnosis of squamous intraepithelial lesions: a meta-analysis," *Obstet. Gynecol.* **91**(4), 626–631 (1998).
4. M. S. Bergholt et al., "Combining near-infrared-excited autofluorescence and Raman spectroscopy improves in vivo diagnosis of gastric cancer," *Biosens. Bioelectron.* **26**(10), 4104–4110 (2011).
5. N. Stone et al., "Near-infrared Raman spectroscopy for the classification of epithelial pre-cancers and cancers," *J. Raman Spectrosc.* **33**(7), 564–573 (2002).
6. S. Duraipandian et al., "In vivo diagnosis of cervical precancer using Raman spectroscopy and genetic algorithm techniques," *Analyst* **136**(20), 4328–4336 (2011).
7. A. Mahadevan-Jansen et al., "Near-infrared Raman spectroscopy for in vitro detection of cervical precancers," *Photochem. Photobiol.* **68**(1), 123–132 (1998).
8. X. Shao, W. Zheng, and Z. Huang, "Near-infrared autofluorescence spectroscopy for in vivo identification of hyperplastic and adenomatous polyps in the colon," *Biosens. Bioelectron.* **30**(1), 118–122 (2011).
9. S. Duraipandian et al., "Simultaneous fingerprint and high-wavenumber confocal Raman spectroscopy enhances early detection of cervical precancer in vivo," *Anal. Chem.* **84**(14), 5913–5919 (2012).
10. Z. Huang et al., "Near-infrared Raman spectroscopy for optical diagnosis of lung cancer," *Int. J. Cancer* **107**(6), 1047–1052 (2003).
11. M. S. Bergholt et al., "In vivo diagnosis of esophageal cancer using image-guided Raman endoscopy and biomolecular modeling," *Technol. Cancer Res. Treat.* **10**(2), 103–112 (2011).
12. Z. Huang et al., "Raman spectroscopy in combination with background near-infrared autofluorescence enhances the in vivo assessment of malignant tissues," *Photochem. Photobiol.* **81**(5), 1219–1226 (2005).
13. Z. Huang et al., "Integrated Raman spectroscopy and trimodal wide-field imaging techniques for real-time in vivo tissue Raman measurements at endoscopy," *Opt. Lett.* **34**(6), 758–760 (2009).
14. X. Shao, W. Zheng, and Z. Huang, "Polarized near-infrared autofluorescence imaging combined with near-infrared diffuse reflectance imaging for improving colonic cancer detection," *Opt. Express* **18**(23), 24293–24300 (2010).

15. X. Shao, W. Zheng, and Z. Huang, "In vivo diagnosis of colonic precancer and cancer using near-infrared autofluorescence spectroscopy and biochemical modeling," *J. Biomed. Opt.* **16**(6), 067005 (2011).
16. J. Mo, W. Zheng, and Z. Huang, "Fiber-optic Raman probe couples ball lens for depth-selected Raman measurements of epithelial tissue," *Biomed. Opt. Express* **1**(1), 17–30 (2010).
17. B. S. Apgar, G. L. Brotzman, and M. Spitzer, *Colposcopy, Principles and Practice : an Integrated Textbook and Atlas*, Saunders/Elsevier, Philadelphia (2008).
18. J. Jeronimo and M. Schiffman, "Colposcopy at a crossroads," *Am. J. Obstet. Gynecol.* **195**(2), 349–353 (2006).
19. S. Duraipandian et al., "Real-time Raman spectroscopy for in vivo, online gastric cancer diagnosis during clinical endoscopic examination," *J. Biomed. Opt.* **17**(8), 081418 (2012).
20. N. Stone et al., "Raman spectroscopy for identification of epithelial cancers," *Faraday Discuss.* **126**, 141–157 (2004).
21. Z. Movasaghi, S. Rehman, and I. U. Rehman, "Raman spectroscopy of biological tissues," *Appl. Spectrosc. Rev.* **42**(5), 493–541 (2007).
22. L. E. Kamemoto et al., "Near-infrared micro-Raman spectroscopy for in vitro detection of cervical cancer," *Appl. Spectrosc.* **64**(3), 255–261 (2010).
23. A. Robichaux-Viehoever et al., "Characterization of Raman spectra measured in vivo for the detection of cervical dysplasia," *Appl. Spectrosc.* **61**(9), 986–993 (2007).
24. J. Wang et al., "Development of a beveled fiber-optic confocal Raman probe for enhancing in vivo epithelial tissue Raman measurements at endoscopy," *Opt. Lett.* **38**(13) (2013).
25. G. Zhang, S. G. Demos, and R. R. Alfano, "Far-red and NIR spectral wing emission from tissues under 532 and 632 nm photo-excitation," *Lasers. Life Sci.* **9**(1), 1–16 (1999).
26. W. Zheng et al., "Optimal excitation-emission wavelengths for autofluorescence diagnosis of bladder tumors," *Int. J. Cancer* **104**(4), 477–481 (2003).
27. L. Coghlan et al., "Optimal fluorescence excitation wavelengths for detection of squamous intra-epithelial neoplasia: results from an animal model," *Opt. Express* **7**(12), 436–446 (2000).
28. D. M. Harris and J. Werkhaven, "Endogenous porphyrin fluorescence in tumors," *Lasers Surg. Med.* **7**(6), 467–472 (1987).
29. W. Lohmann et al., "Native fluorescence of the cervix uteri as a marker for dysplasia and invasive carcinoma," *Eur. J. Obstet. Gynecol. Reprod. Biol.* **31**(3), 249–253 (1989).
30. R. Drezek et al., "Understanding the contributions of NADH and collagen to cervical tissue fluorescence spectra: modeling, measurements, and implications," *J. Biomed. Opt.* **6**(4), 385–396 (2001).
31. S. K. Chang et al., "Analytical model to describe fluorescence spectra of normal and preneoplastic epithelial tissue: comparison with Monte Carlo simulations and clinical measurements," *J. Biomed. Opt.* **9**(3), 511–522 (2004).
32. F. Lyng et al., "Vibrational spectroscopy for cervical cancer pathology, from biochemical analysis to diagnostic tool," *Exp. Mol. Pathol.* **82**(2), 121–129 (2007).
33. P. R. T. Jess et al., "Early detection of cervical neoplasia by Raman spectroscopy," *Int. J. Cancer* **121**(12), 2723–2728 (2007).
34. R. Richards-Kortum and E. Sevick-Muraca, "Quantitative optical spectroscopy for tissue diagnosis," *Annu. Rev. Phys. Chem.* **47**, 555–606 (1996).
35. D. R. Velez et al., "A balanced accuracy function for epistasis modeling in imbalanced datasets using multifactor dimensionality reduction," *Genet. Epidemiol.* **31**(4), 306–315 (2007).